Pt-Containing High-Entropy Oxide Confined in SBA-15 for Efficient Extractive–Oxidative Desulfurization

Ruoyu Liu,[a,b,#] Weimin Zhai,[b,d,#] Jiahui Li,[a] Linlin Chen,[a] Peng Cui,[a] Zhendong Yu,[b] Wenshuai Zhu,[a,b,c,*] Peiwen Wu[a,b,*]

[a]School of Chemistry and Chemical Engineering, Jiangsu University, Zhenjiang, 212013, PR China

[b]College of Chemical Engineering and Environment, State Key Laboratory of Heavy Oil Processing, China University of Petroleum-Beijing, Beijing, 102249, PR China

[c]Shandong Key Laboratory of Green Electricity & Hydrogen Science and Technology, Shandong Institute of Petroleum and Chemical Technology, Dongying 257061, PR China

[d]SINOPEC Research Institute of Petroleum Processing Co., Ltd., Beijing 100083, PR China

[#]These two authors contributed equally.

*Corresponding authors: Wenshuai Zhu (zhuws@cup.edu.cn); Peiwen Wu (wupeiwen@ujs.edu.cn)

Table S1 Physicochemical parameters of metal elements selected for constructing the HEO

Metal	Atomic radius (Å)	Oxidation state	Ionic radius (Å)
Pt	~1.28	+2/+4	~0.76
Fe	~1.25	+3	~0.78
Co	~1.26	+2/+3	~0.74
Ni	~1.21	+2	~0.69
Cu	~1.28	+2	~0.73

Table S2 Elemental composition of the HEO(Pt)@SBA-15 catalyst determined by ICP analysis

Element	Concentration in diluted solution (mg L^{-1})	Content in catalyst (mg L^{-1})
Pt	1.5729	15.73
Fe	1.5717	15.72
Co	0.1057	1.06
Ni	0.3812	3.81
Cu	1.0472	10.47

Note: The catalyst (40 mg) was completely dissolved in 8 mL of aqua regia. An aliquot of 0.2 mL of the solution was diluted 50 times prior to ICP analysis. The elemental contents were calculated based on the total digestion volume and catalyst mass.

Table S3 N_2 adsorption-desorption parameters for porous frameworks.

Porous framework	**Specific surface area** （$m^2 g^{-1}$）	**Bore volume** （$cm^3 g^{-1}$）	**Average pore size** （nm）
SBA-15	570.7	0.873	6.02
HEO(Pt)@SBA-15	427.8	1.008	9.05

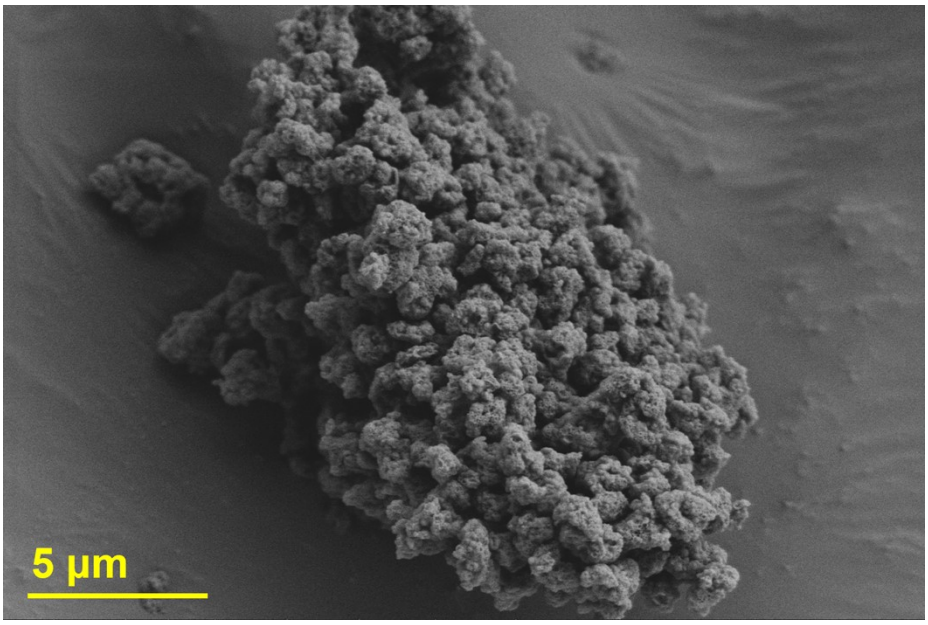

Fig. S1 Magnified SEM image of HEO(Pt)@SBA-15.

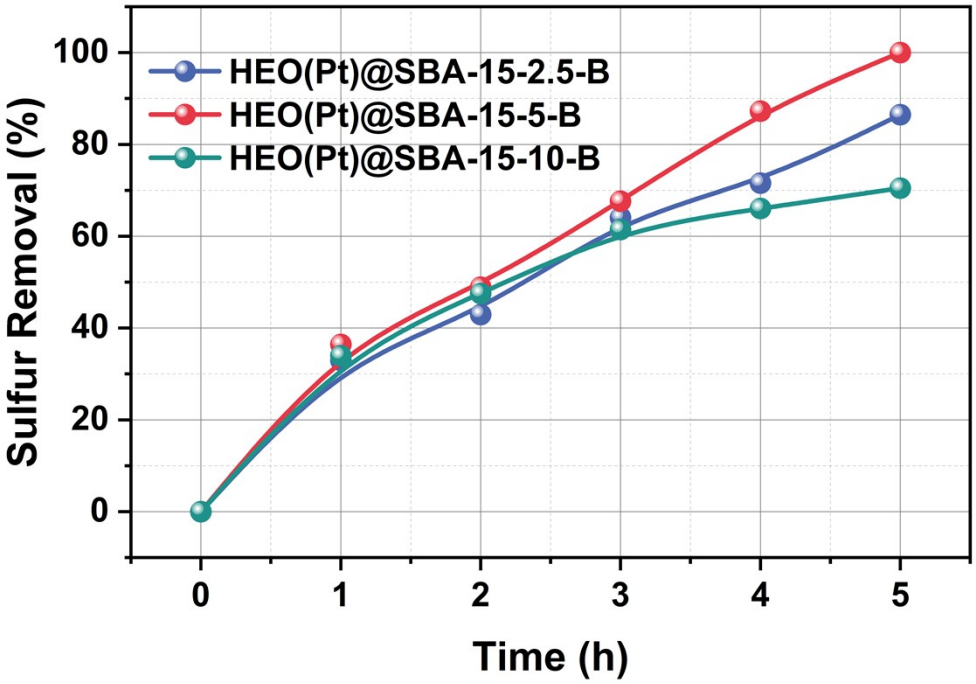

Fig. S2 Catalytic oxidation performance of HEO(Pt)@SBA-15-2.5-B, HEO(Pt)@SBA-15-5-B and HEO(Pt)@SBA-15-10-B. Reaction conditions: *V*(model oil, DBT: S 200 μg g^{-1}) = 20 mL; *T* = 130°C; *V*(cat) = 4 mL; *v*(O_2) = 200 mL min^{-1}.

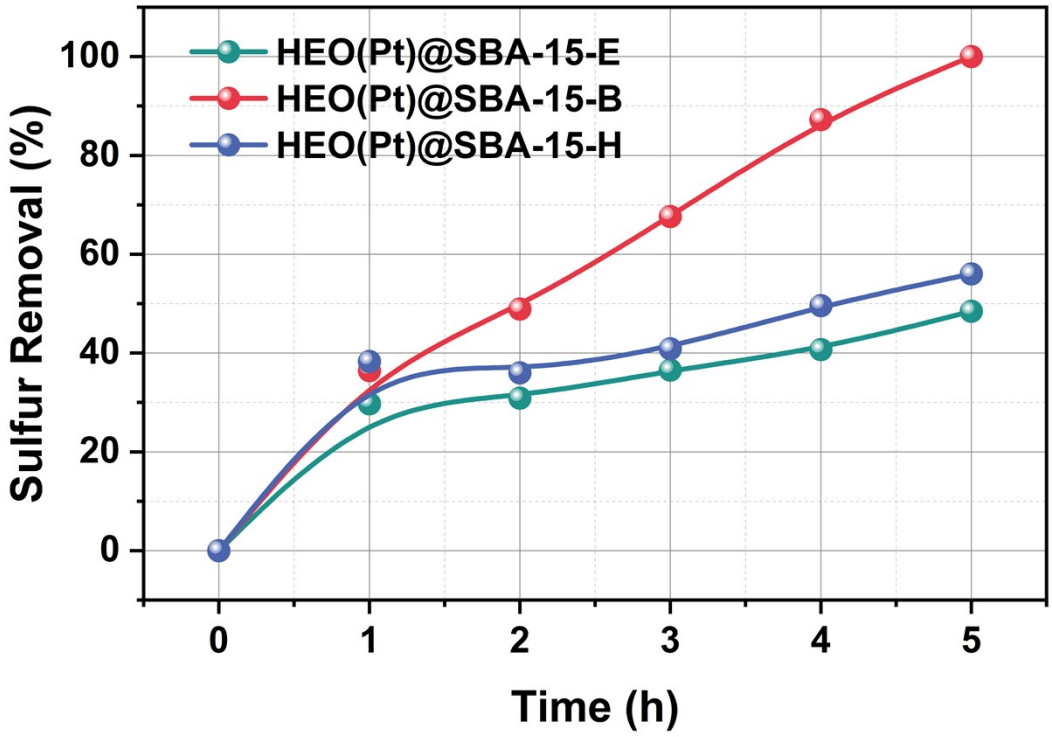

Fig. S3 Catalytic oxidation performance of HEO(Pt)@SBA-15-B, HEO(Pt)@SBA-15-E and HEO(Pt)@SBA-15-O. Reaction conditions: *V*(model oil, DBT: S 200 μg g^{-1}) = 20 mL; *T* = 130°C; *V*(cat.) = 4 mL; *v*(O_2) = 200 mL min^{-1}.

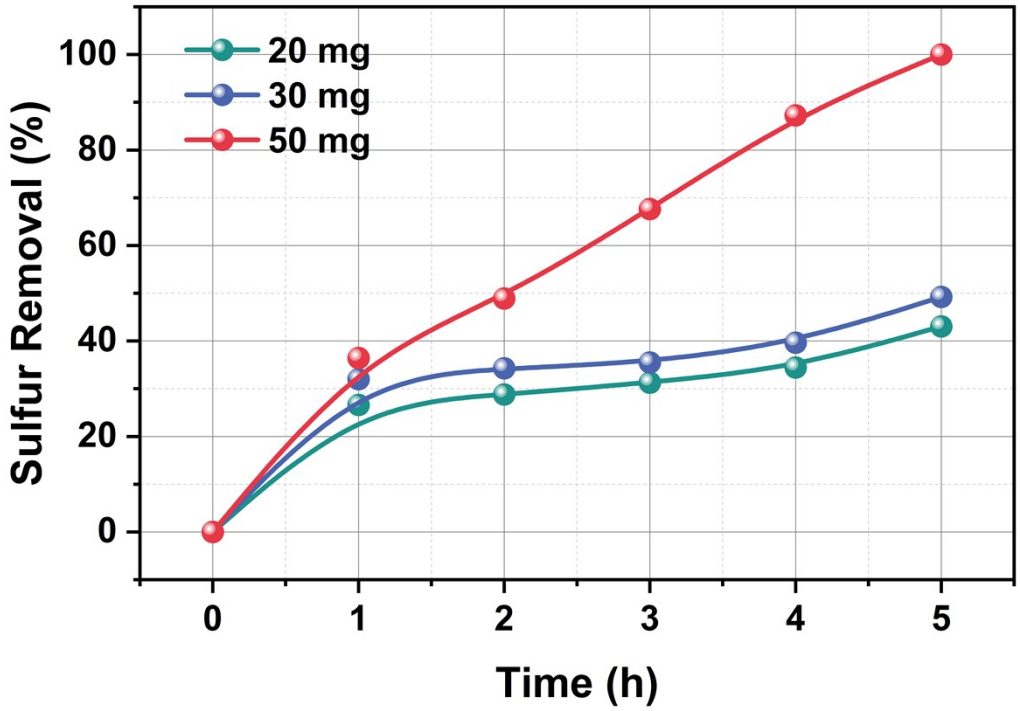

Fig. S4 Different HESAC@SBA-15 dosages (per 4 mL of [Bmim]BF_4). Reaction conditions: *V*(model oil, DBT: S 200 μg g^{-1}) = 20 mL; *T* = 130°C; *V*(HEO(Pt)@SBA-15-B) = 4 mL; *v*(O_2) = 200 mL min^{-1}.

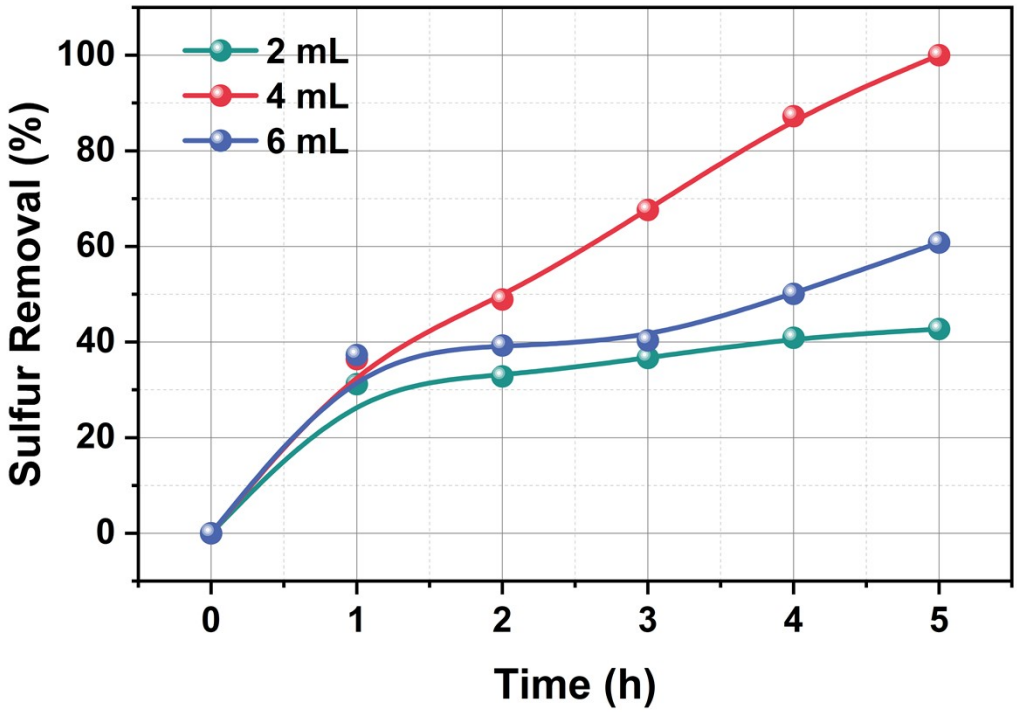

Fig. S5 Different HEO(Pt)@SBA-15-B dosages. Reaction conditions: *V*(model oil, DBT: S 200 μg g^{-1}) = 20 mL; *T* = 130°C; *v*(O_2) = 200 mL min^{-1}.

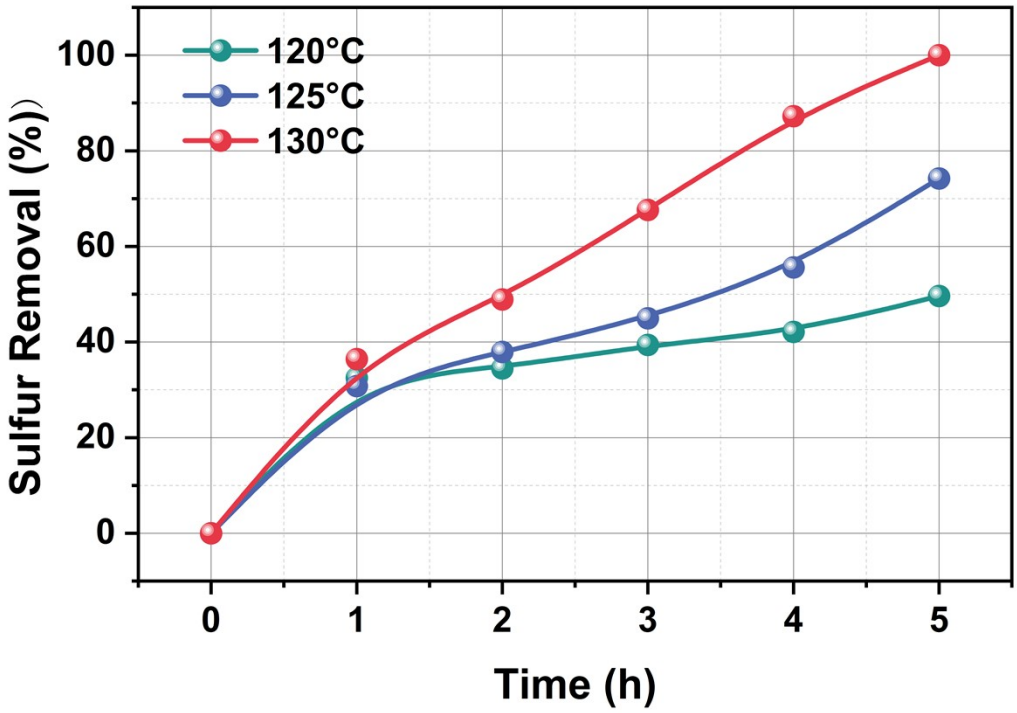

Fig. S6 Different reaction temperatures. Reaction conditions: *V*(model oil, DBT: S 200 μg g^{-1}) = 20 mL; *V*(HEO(Pt)@SBA-15-B) = 4 mL; *v*(O_2) = 200 mL min^{-1}.

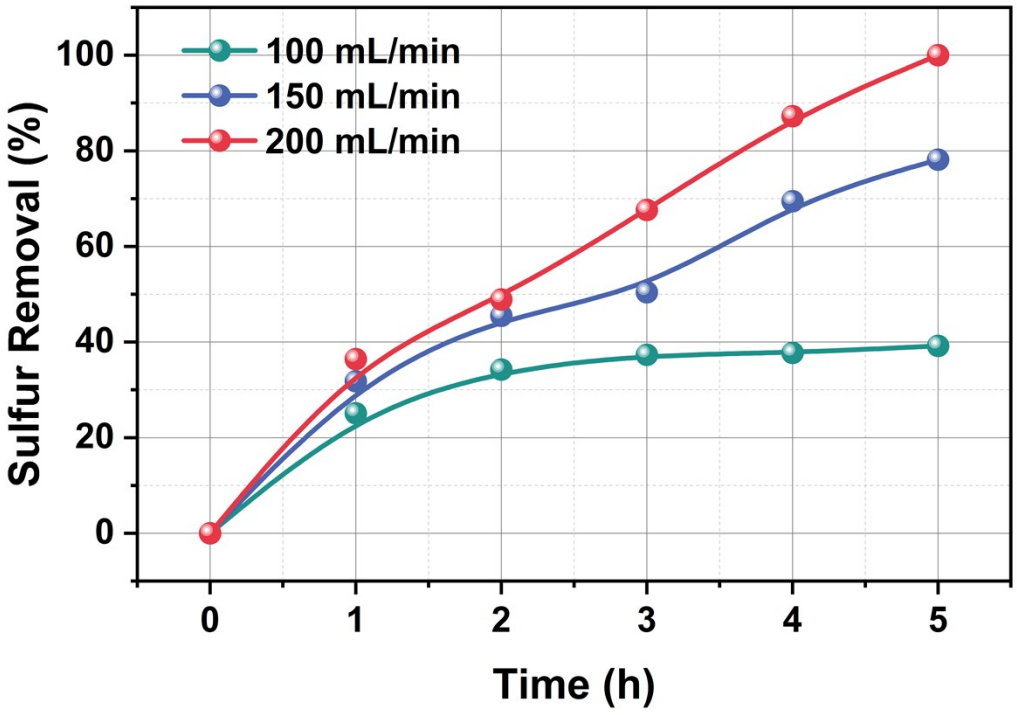

Fig. S7 Different oxygen fluxes. Reaction conditions: *V*(model oil, DBT: S 200 μg g^{-1}) = 20 mL; *T* = 130°C; *V*(HEO(Pt)@SBA-15-B) = 4 mL

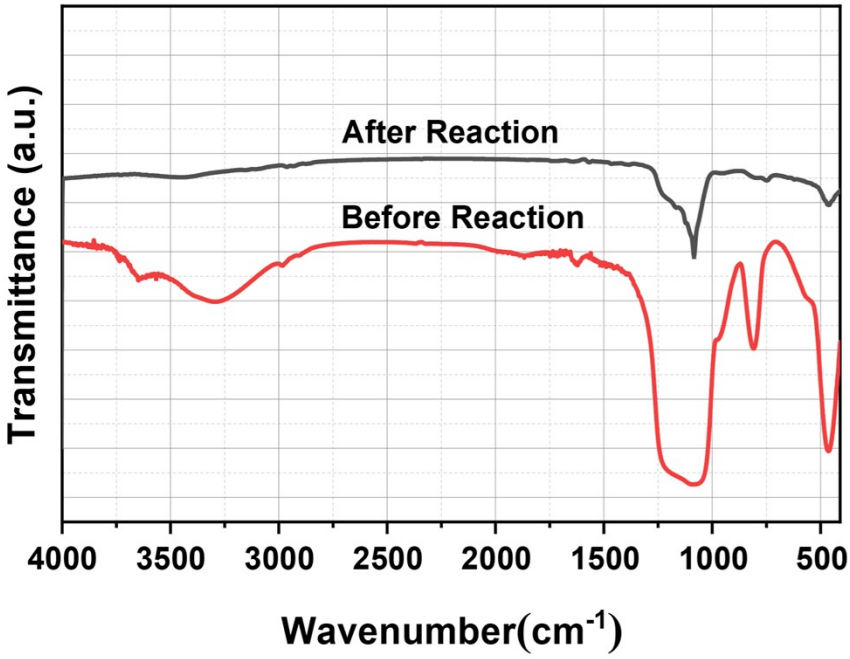

Fig. S8 FT-IR comparison of HEO(Pt)@SBA-15 before and after reaction.

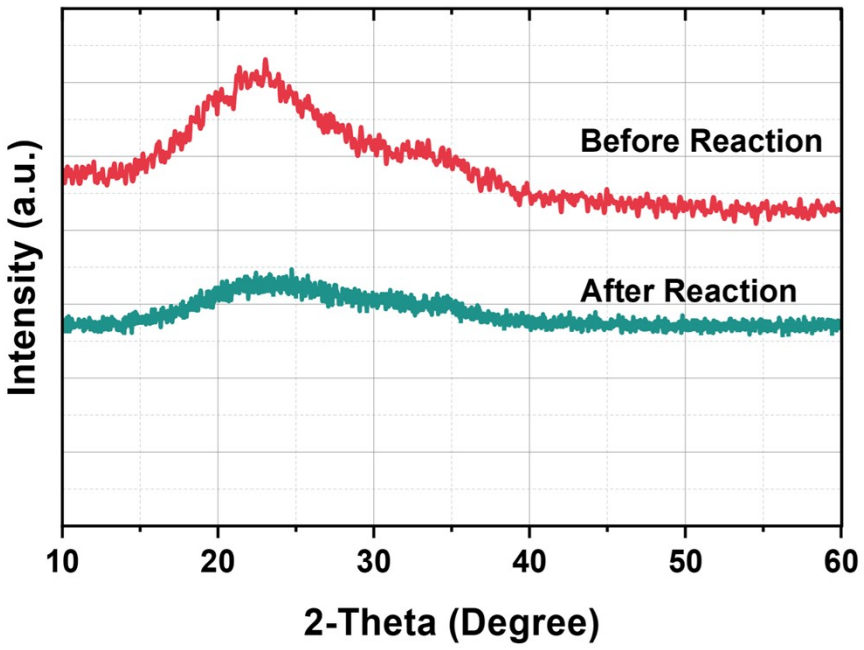

Fig. S9 XRD comparison of HEO(Pt)@SBA-15 before and after reaction.

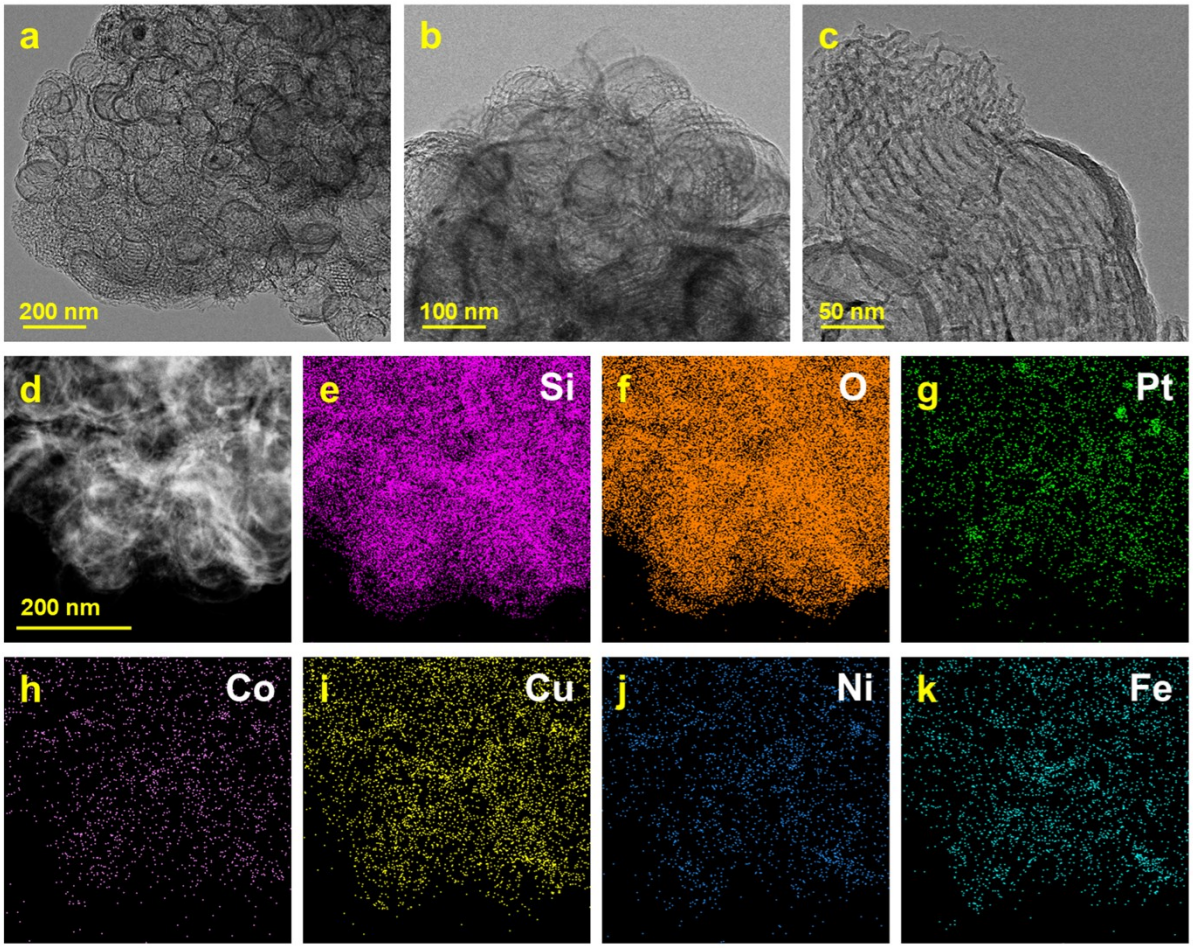

Fig. S10 Electron microscopy characterization and corresponding elemental EDS mapping of HEO(Pt)@SBA-15 after reaction.

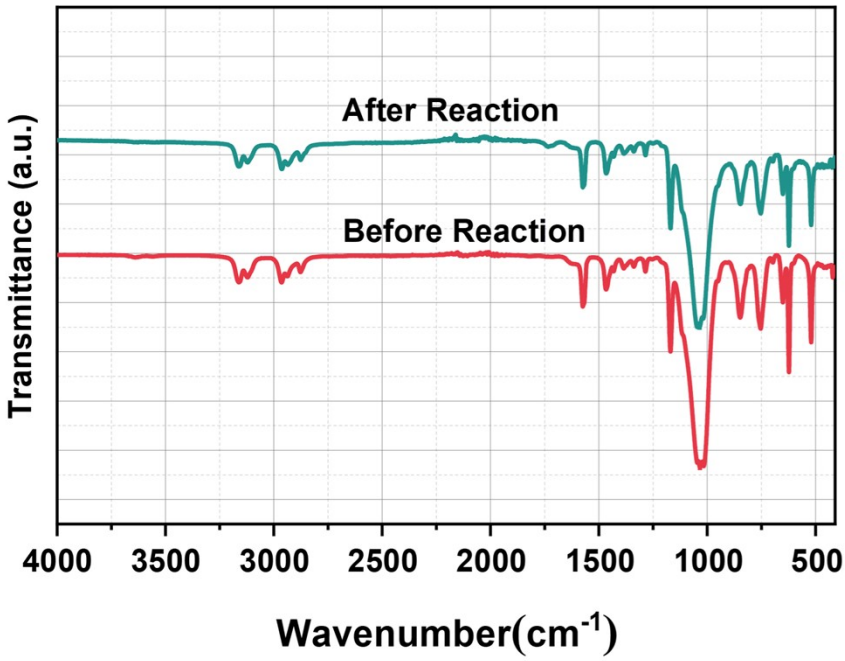

Fig. S11 FT-IR comparison of HEO(Pt)@SBA-15-B before and after reaction.

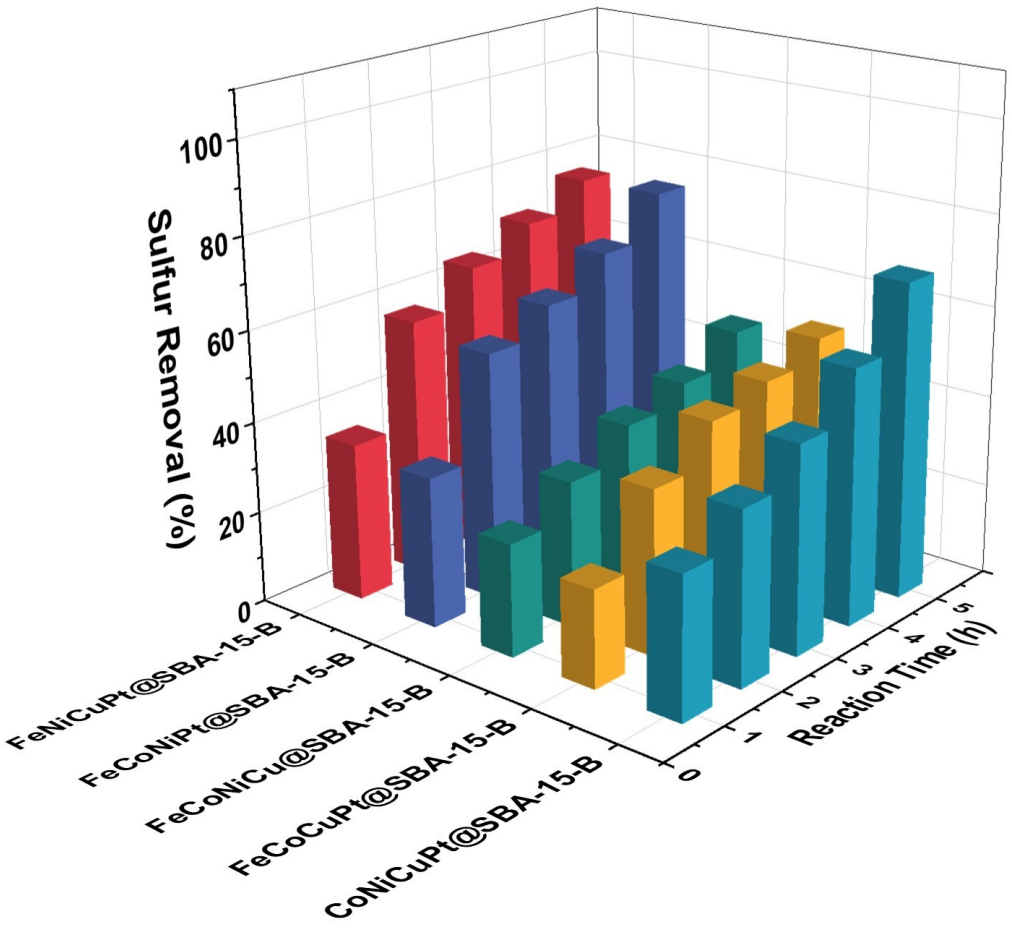

Fig. S12 Determination of catalytically active sites by investigating MEO@SBA-15 as catalyst. Reaction conditions: *V*(model oil, DBT: S = 200 μg g^{-1}) = 20 mL; *T* = 130°C; *V*(HEO(Pt)@SBA-15-B) = 4 mL; *v*(O_2) = 200 mL min^{-1}.

Table S4 Benchmark comparison of representative ECODS systems for oxidative desulfurization of DBTs

Catalysts	Oxidant	T/°C	t/min	Sulfur removal/%	Ref.
HEO(Pt)@SBA-15-B	O_2	130	300	100	This work
HPA-5	O_2	130	720	100	[1]
$C_{16}PMoV/10SiO_2$	O_2	120	300	96.4	[2]
$[(C_{18}H_{37})_2N(CH_3)_2]_5[IMo_6O_{24}]$	O_2	80	480	100	[3]
$CrMo_6$ -PEG/SSA	O_2	60	240	~100	[4]
Mo-NIFs	H_2O_2	60	40	97.9	[5]
UiO-66-T3PILs	H_2O_2	50	240	95.3	[6]
$[C_2(MIM)_2]PW_{12}O_{40}$	H_2O_2	50	60	98	[7]

References

1. B. Bertleff, J. Claußnitzer, W. Korth, P. Wasserscheid, A. Jess and J. Albert, *Energy & Fuels*, 2018, **32**, 8683-8688.
2. Q. Wang, T. Huang, S. Tong, C. Wang, H. Li and M. Zhang, *Molecules*, 2024, **29.**
3. H. Lü, Y. Zhang, Z. Jiang and C. Li, *Green Chemistry*, 2010, **12**, 1954.
4. M. Chi, Z. Zhu, L. Sun, T. Su, W. Liao, C. Deng, Y. Zhao, W. Ren and H. Lü, *Applied Catalysis B: Environmental*, 2019, **259**, 118089.
5. X. Zhang, J. Zhang, J. Yin, X. Liu, W. Qiu, J. He, W. Jiang, L. Zhu, H. Li and H. Li, *Sep. Purif. Technol.*, 2025, **353**, 128289.
6. J. Yin, W. Fu, J. Zhang, X. Liu, X. Zhang, C. Wang, J. He, W. Jiang, H. Li and H. Li, *Chem. Eng. J.*, 2023, **470**, 144290.
7. J. Li, Y. Guo, J. Tan and B. Hu, *Catalysts*, 2021, **11**, 356.